GAMMA RADIATION FROM THE REACTIONS $^{20}Ne(\alpha, \alpha'\gamma_{1\cdot63})^{20}Ne$ AND $^{20}Ne(\alpha, p\gamma_{0\cdot44})^{23}Na$

By R. H. Spear* and I. F. Wright†

[*Manuscript received January* 5, 1968]

Summary

Excitation functions for γ-radiation from the reactions $^{20}Ne(\alpha, \alpha'\gamma_{1\cdot63})^{20}Ne$ and $^{20}Ne(\alpha, p\gamma_{0\cdot44})^{23}Na$ have been studied for bombarding energies from 3·96 to 6·08 MeV. Angular distribution measurements provide spin and parity assignments of 2^+ for ^{24}Mg levels at excitation energies of 12·74 and 12·81 MeV, and 4^+ or 5^- (possibly 6^+) for a level at 12·98 MeV.

I. Introduction

This paper reports a survey of the excitation functions for 1·63 and 0·44 MeV γ-rays from the reactions $^{20}Ne(\alpha, \alpha'\gamma_{1\cdot63})^{20}Ne$ and $^{20}Ne(\alpha, p\gamma_{0\cdot44})^{23}Na$; the work was undertaken to obtain new information on the level structure of ^{24}Mg at excitation energies of about 13 MeV. Data were taken at 55° for α-particle energies E_α from 5·21 to 6·08 MeV, and at 0°, 90°, and 125° for E_α from 3·96 to 5·25 MeV. The α-particle energies from 3·96 to 6·08 MeV correspond to excitation energies E_x in ^{24}Mg from 12·61 to 14·37 MeV. This region of ^{24}Mg has been previously studied from several reactions. Extensive investigations of states populated in the proton bombardment of ^{23}Na have been made by a number of authors (see Endt and Van der Leun 1962); collectively these extend up to $E_x = 14\cdot0$ MeV. The reaction $^{20}Ne(\alpha, \gamma)^{24}Mg$ has recently been studied by Highland and Thwaites (1967) for α-particle energies from 3 to 6 MeV. Ollerhead and Kuehner (1965) and McGough and Wright (personal communication) have studied some states in the region using the reaction $^{12}C(^{16}O, \alpha)^{24}Mg$.

Both ^4He and ^{20}Ne have zero spin and even parity; therefore α-particle bombardment of ^{20}Ne can populate only natural parity states of ^{24}Mg, i.e. $J^\pi = 0^+$, 1^-, 2^+, 3^-, 4^+, etc. For the reaction $^{20}Ne(\alpha, \alpha'\gamma_{1\cdot63})^{20}Ne$, the angular momentum situation is relatively simple; since barrier-penetrability considerations are expected to limit the orbital angular momentum of the outgoing α-particle to the two lowest possible values, straightforward γ-ray angular distribution measurements may provide unambiguous J^π values for ^{24}Mg states.

II. Experimental Procedure

Beams of singly and doubly ionized helium were obtained from the Australian National University tandem accelerator. The ^{20}Ne target‡ was prepared in an

* Research School of Physical Sciences, Australian National University, Canberra, A.C.T. 2600.

† University of Manchester, Manchester, England.

‡ Supplied by the Electromagnetic Separation Group, A.E.R.E., Harwell, England.

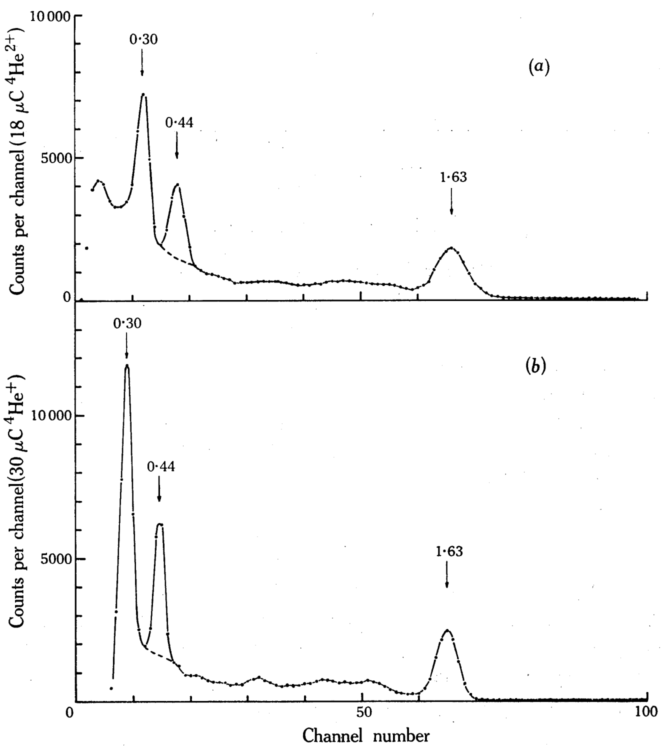

Fig. 1.—Typical γ-ray spectra from α-particle bombardment of ^{20}Ne for (a) $E_\alpha = 5 \cdot 80$ MeV, $12 \cdot 7$ cm diameter by $10 \cdot 2$ cm long crystal, and 55°; (b) $E_\alpha = 5 \cdot 25$ MeV, $7 \cdot 6$ cm diameter by $7 \cdot 6$ cm long crystal, and 0°.

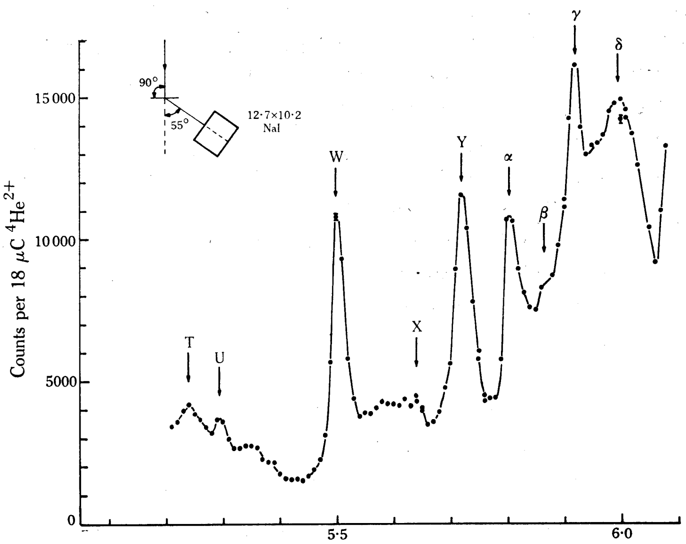

Fig. 2.—Excitation function for $1 \cdot 63$ MeV γ-radiation from $^{20}Ne(\alpha, \alpha'\gamma_{1 \cdot 63})^{20}Ne$ at 55° for $5 \cdot 21 < E_\alpha < 6 \cdot 08$ MeV.

electromagnetic isotope separator by ion bombardment at 30 kV onto a 0·025 mm tantalum foil. It had a nominal loading of 5 μg/cm^2. The target was supported by a backing of 0·56 mm tantalum on the vertical axis of a cylindrical glass target chamber. In order to minimize beam deposition of carbon, the target was surrounded by a cylindrical copper sleeve maintained at liquid nitrogen temperature (Bashkin and Ophel 1962). Tantalum collimators were used to produce a beam spot of approximately 3 mm diameter on the target. Beam currents ranged from about 0·1 to 0·3 μA. Precautions were taken to suppress secondary electrons, and current integration was accurate to about 1%.

Gamma rays were detected using NaI(Tl) crystals. For α-particle energies E_α from 5·21 to 6·08 MeV, a single 12·7 cm diameter by 10·2 cm long crystal was set at 55° to the beam axis with h, the distance of the front face of the crystal from the target spot, equal to 9·51 cm. For E_α from 3·96 to 5·25 MeV, 7·6 cm diameter by 7·6 cm long crystals were set at 0° and 125° ($h = 7 \cdot 43$ and 7·38 cm respectively) and a 12·7 cm diameter by 10·2 cm long crystal was set at 90° ($h = 12 \cdot 03$ cm). Pulses were analysed using standard electronics and displayed on 400-channel pulse height analysers.

III. Excitation Functions

Two typical γ-ray spectra are shown in Figure 1 for (*a*) $E_\alpha = 5 \cdot 80$ MeV, 12·7 cm by 10·2 cm crystal, and 55°; and (*b*) $E_\alpha = 5 \cdot 25$ MeV, 7·6 cm by 7·6 cm crystal, and 0°. Gamma rays of energies 1·63, 0·44, and 0·30 MeV are clearly evident in both spectra.

The 0·44 MeV radiation is attributed to the reaction ^{20}Ne(α, p$\gamma_{0.44}$)^{23}Na proceeding via the $\frac{5}{2}^+$ first excited state of ^{23}Na. Sodium contamination of the target or beam collimators could produce 0·44 MeV radiation through the reaction ^{23}Na(α, $\alpha'\gamma_{0.44}$)^{23}Na. The complete absence of any 1·81 MeV radiation (from the reaction ^{23}Na(α, p$\gamma_{1.81}$)^{26}Mg) shows that such contamination was negligible.

The 1·63 MeV radiation is attributed to the reaction ^{20}Ne(α, $\alpha'\gamma_{1.63}$)^{20}Ne proceeding via the 2$^+$ first excited state of ^{20}Ne. For E_α greater than 5·35 MeV the reaction ^{20}Ne(α, p)^{23}Na* (2·08 MeV) is energetically possible and would produce γ-radiation of energies 1·64, 0·44, and 2·08 MeV. The absence of any observable 2·08 MeV radiation shows that this reaction did not contribute any significant background to the yields of the two reactions studied.

The 0·30 MeV radiation comes from Coulomb excitation of ^{181}Ta (Vivargent 1959).

Excitation functions for 1·63 MeV radiation are shown in Figures 2 and 3. For $5 \cdot 21 < E_\alpha < 6 \cdot 08$ MeV (Fig. 2), the target surface was perpendicular to the beam direction, and the ordinate represents the number of pulses within a window from 1·50 to 1·76 MeV for a bombardment equivalent to 18 μC ^{4}He^{2+}. For $3 \cdot 96 < E_\alpha < 5 \cdot 25$ MeV (Fig. 3), the target surface was at 45° to the beam direction, and the ordinate represents the number of pulses within a window from 1·50 to 1·79 MeV for a bombardment equivalent to 30 μC ^{4}He$^+$. In each case small corrections have been made for dead-time losses (< 3%), room background, and pulses within the window arising from higher energy radiation produced by the beam. Statistical error bars are indicated at 100 keV intervals, except in cases where they are smaller than the size of the data points.

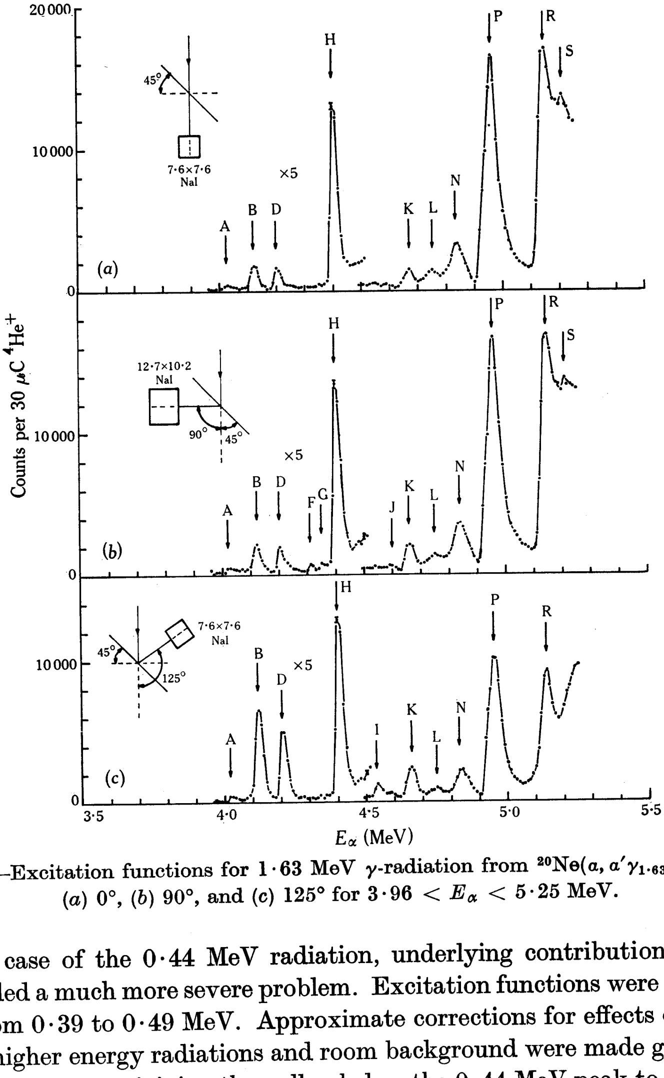

Fig. 3.—Excitation functions for $1 \cdot 63$ MeV γ-radiation from $^{20}Ne(\alpha, \alpha'\gamma_{1 \cdot 63})^{20}Ne$ at (a) 0°, (b) 90°, and (c) 125° for $3 \cdot 96 < E_\alpha < 5 \cdot 25$ MeV.

In the case of the $0 \cdot 44$ MeV radiation, underlying contributions from other γ-rays provided a much more severe problem. Excitation functions were derived using a window from $0 \cdot 39$ to $0 \cdot 49$ MeV. Approximate corrections for effects of underlying pulses from higher energy radiations and room background were made graphically by drawing a smooth curve joining the valley below the $0 \cdot 44$ MeV peak to the spectrum extending above the $0 \cdot 44$ MeV peak; examples are shown by the dashed lines in Figure 1. This procedure is admittedly rather subjective, and the fraction of the total $0 \cdot 44$ MeV spectrum accepted depends on the intensity and slope of the underlying spectrum. Nevertheless, it gives a reasonably good representation of the gross features of the excitation function; peak positions are certainly significant, but the yields in the valleys between peaks may be somewhat unreliable. Dead-time corrections have been applied. Results are shown in Figure 4 ($5 \cdot 21 < E_\alpha < 6 \cdot 08$ MeV, 18 μC $^4He^{2+}$) and Figure 5 ($3 \cdot 96 < E_\alpha < 5 \cdot 25$ MeV, 30 μC $^4He^+$).

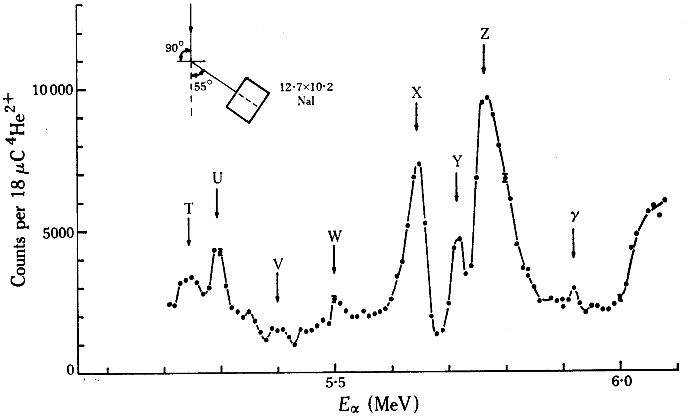

Fig. 4.—Excitation function for 0·44 MeV γ-radiation from $^{20}Ne(\alpha, p\gamma_{0\cdot44})^{23}Na$ at 55° for $5\cdot21 < E_\alpha < 6\cdot08$ MeV.

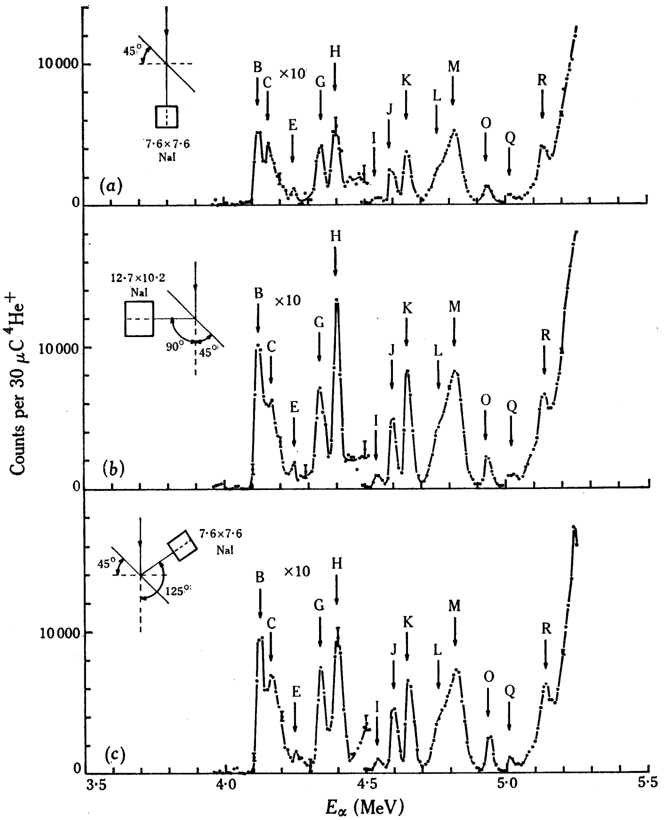

Fig. 5.—Excitation functions for 0·44 MeV γ-radiation from $^{20}Ne(\alpha, p\gamma_{0\cdot44})^{23}Na$ at (a) 0°, (b) 90°, and (c) 125° for $3\cdot96 < E_\alpha < 5\cdot25$ MeV.

For ease of reference, peaks in the excitation functions in Figures 2–5 are labelled alphabetically. The energies of peaks for $E_\alpha < 4 \cdot 6$ MeV are listed with the corresponding ^{24}Mg excitation energies in Table 1. Individual peaks for E_α greater than $4 \cdot 6$ MeV are not listed because most of them are probably due to more than one level in ^{24}Mg. It is assumed that $E_x = (9 \cdot 317 + 0 \cdot 833\, E_\alpha)$ MeV. Uncertainties in the values of E_x and E_α are conservatively estimated at ± 13 and ± 15 keV respectively. The resonance energies listed represent averages from all angles at which the peaks were observed.

Table 1

RESONANCE ENERGIES (E_α) AND EXCITATION ENERGIES (E_x) OF ^{24}Mg STATES OBSERVED IN $^{20}\mathrm{Ne}(\alpha, \alpha'\gamma_{1\cdot 63})^{20}\mathrm{Ne}$ AND $^{20}\mathrm{Ne}(\alpha, \mathrm{p}\gamma_{0\cdot 44})^{23}\mathrm{Na}$

Assuming that each peak observed in the excitation function corresponds to a state in ^{24}Mg

Peak	1·63 MeV Radiation E_α* (MeV)	1·63 MeV Radiation E_x† (MeV)	0·44 MeV Radiation E_α* (MeV)	0·44 MeV Radiation E_x† (MeV)
A	4·022	12·667		
B	4·115	12·745	4·115	12·745
C			4·158‡	12·781
D	4·195	12·811		
E			4·245	12·853
F	4·305	12·903		
G	4·345	12·936	4·338	12·931
H	4·395	12·978	4·395	12·978
I	4·535	13·095	4·535	13·095
J	4·590	13·140	4·593	13·143

* All values are $\pm 0 \cdot 015$ MeV.

† All values are $\pm 0 \cdot 013$ MeV.

‡ If this peak is due to a single level, the level width is 28 ± 9 keV.

Using narrow resonances in $^{20}\mathrm{Ne}(\alpha, \gamma)^{24}\mathrm{Mg}$, the target thickness was measured as 24 ± 5 keV and 21 ± 5 keV at $E_\alpha = 3 \cdot 05$ and $6 \cdot 08$ MeV respectively. These values show that the widths of all the peaks listed in Table 1 (with the exception of peak C) can be attributed entirely to the target thickness.

IV. Angular Distributions

As noted in Section I, the angular momentum situation for the reaction $^{20}\mathrm{Ne}(\alpha, \alpha'\gamma_{1\cdot 63})^{20}\mathrm{Ne}$ is sufficiently simple that in some circumstances γ-ray angular distribution measurements are sufficient to give unambiguous spin and parity assignments for the ^{24}Mg state involved. Yield ratios of $1 \cdot 63$ MeV radiation obtained from the crystals at 0°, 90°, and 125° have been compared with theoretical ratios in an attempt to determine spins and parities for some of the lower energy resonances. No angular distribution analysis has been attempted for the $0 \cdot 44$ MeV radiation because of (1) the non-unique channel spin and (2) the difficulty of assessing background reliably.

The angular distribution of 1·63 MeV radiation will have the form

$$W(\theta) = 1+Q_2 A_2 P_2(\cos\theta) + Q_4 A_4 P_4(\cos\theta),$$

where the A's are the theoretical coefficients for perfect geometry and the Q's are the attenuation coefficients that correct for finite geometry. For the case in which the compound ^{24}Mg state has well-defined spin and parity, the theoretical coefficients can be readily calculated for particular values of l', the orbital angular momentum of the outgoing α-particle; if there are contributions from more than one value of l', these contributions add incoherently (Kraus *et al.* 1956). In the energy range considered here the energies of the emitted α-particles are low compared with the Coulomb and centrifugal barriers, so that only the two lowest possible values of l' will contribute appreciably. Theoretical angular distribution coefficients were calculated for all possible values of J^π and l' up to $J^\pi = 6+$. Corrections for finite geometry were made using angular attenuation coefficients deduced from the values calculated by Yates (1965). The consequent ratios of yields for the three angles used are given in Table 2.

TABLE 2

THEORETICAL YIELD RATIOS OF 1·63 MeV GAMMA RADIATION CORRECTED FOR FINITE GEOMETRY

(1) J^π, l'	(2) $W(90°)/W(0°)$	(3) $W(90°)/W(125°)$	(1) J^π, l'	(2) $W(90°)/W(0°)$	(3) $W(90°)/W(125°)$
0+, 2	1·00	1·00	4+, 2	0·56	0·61
1−, 1	0·53	0·77	4+, 4	3·25	0·84
1−, 3	0·83	0·94	4+, 6	0·72	0·86
2+, 0	0·53	0·15	5−, 3	0·58	0·66
2+, 2	1·83	0·83	5−, 5	3·61	0·84
2+, 4	0·77	0·90	5−, 7	0·71	0·85
3−, 1	0·53	0·51	6+, 4	0·59	0·68
3−, 3	2·70	0·84	6+, 6	3·81	0·84
3−, 5	0·74	0·88	6+, 8	0·70	0·85

The relative efficiencies of the three crystals for the geometry used were determined from the yields observed for the isotropic 1·77 MeV γ-rays emitted in the decay of ^{28}Al (half-life 2·28 min). The ^{28}Al was produced via the reaction ^{25}Mg(α, p)^{28}Al using a thick target of natural magnesium. The results obtained were adjusted to give the relative efficiencies for 1·63 MeV radiation by taking account of the variation with energy of the intrinsic crystal efficiencies and of absorption in materials surrounding the target.

From these efficiencies relative yields of 1·63 MeV γ-radiation have been calculated for all data points in peaks B, D, H, K, N, and P. For peaks B, D, H, and N the angular distributions remained constant across the peak and the mean values are given in Table 3. The errors quoted are a combination of statistical errors and an allowance for geometrical errors due to variations in beam spot position and uncertainty about the relative positions of the ^{20}Ne and magnesium targets. For peaks K and P the angular distributions varied across the peak, indicating that they are not due to single levels.

Comparison of Tables 2 and 3 shows that the results for peaks B and D are in very good agreement with $J^\pi = 2^+$, $l' = 0$, with a small admixture of $l' = 2$. For both peaks no other value of J^π is consistent with the data. The data for peak H fit equally well to $(J^\pi, l') = (4^+, 2)$, $(5^-, 3)$, or $(6^+, 4)$; they exclude values of J less than 4.

Table 3

EXPERIMENTAL YIELD RATIOS FOR 1·63 MeV GAMMA RADIATION

(1) Peak	(2) $W(90°)/W(0°)$	(3) $W(90°)/W(125°)$	(1) Peak	(2) $W(90°)/W(0°)$	(3) $W(90°)/W(125°)$
B	$0\cdot58 \pm 0\cdot04$	$0\cdot20 \pm 0\cdot01$	H	$0\cdot56 \pm 0\cdot03$	$0\cdot66 \pm 0\cdot02$
D	$0\cdot66 \pm 0\cdot05$	$0\cdot25 \pm 0\cdot02$	N	$0\cdot60 \pm 0\cdot03$	$1\cdot04 \pm 0\cdot04$

Although the angular distribution for peak N remained fairly constant across the peak, the results cannot be fitted to any of the theoretical distributions for $J \leqslant 6$. The peak is quite broad and not well resolved; it seems likely that this peak also is complex.

V. Partial Widths

Estimates of $(2J+1)\Gamma_{\alpha_0}\Gamma_{\alpha_1}/\Gamma$ and $(2J+1)\Gamma_{\alpha_0}\Gamma_{p_1}/\Gamma$ for some of the lower energy resonances are listed in Table 4; here Γ_{α_0} is the partial width of the state for emission of ground state α-particles, Γ_{α_1} is the partial width for emission of α-particles to the 1·63 MeV state of ^{20}Ne, and Γ_{p_1} is the partial width for emission of protons to the 0·44 MeV state of ^{23}Na. The results are derived from the 125° data, assuming in each case that the peak height represents the thick target yield. Absolute values were

Table 4

SUMMARY OF PARTIAL WIDTH INFORMATION FOR SOME RESONANCES OBSERVED IN $^{20}\mathrm{Ne}(\alpha, \alpha'\gamma_{1\cdot63})^{20}\mathrm{Ne}$ AND $^{20}\mathrm{Ne}(\alpha, p\gamma_{0\cdot44})^{23}\mathrm{Na}$

(1) Peak	(2) $(2J+1)\Gamma_{\alpha_0}\Gamma_{\alpha_1}/\Gamma$ (eV)	(3) $(2J+1)\Gamma_{\alpha_0}\Gamma_{p_1}/\Gamma$ (eV)	(1) Peak	(2) $(2J+1)\Gamma_{\alpha_0}\Gamma_{\alpha_1}/\Gamma$ (eV)	(3) $(2J+1)\Gamma_{\alpha_0}\Gamma_{p_1}/\Gamma$ (eV)
A	60	$\lesssim 10$	E	$\lesssim 40$	30
B	800*	270	G	50	205
C	$\lesssim 45$	185	H	2050*	270
D	600*	$\lesssim 100$	I	600	230

* Corrected for angular distribution effects.

obtained by comparing observed yields with the yield of ground state γ-rays obtained from the reaction $^{20}\mathrm{Ne}(\alpha, \gamma)^{24}\mathrm{Mg}$ at the 3·05 MeV resonance; measurements by Smulders (1965) indicate that for this resonance $J^\pi = 1^-$ and $\Gamma_{\gamma_0} = 0\cdot5$ eV. Values for B, D, and H in column 2 of Table 4 have been corrected for angular distribution effects; it is estimated that they are accurate to $\pm 40\%$. Other values are probably accurate to within a factor of two. The results of Table 4 do not give Γ_{α_1} and Γ_{p_1} explicitly; however, since $\Gamma > \Gamma_{\alpha_0}$, they may be used to set a lower limit on $(2J+1)\Gamma_{\alpha_1}$ and $(2J+1)\Gamma_{p_1}$.

VI. Discussion

In discussing these results it is convenient to divide the energy range covered at an α-particle energy of 4·6 MeV. Above this energy many of the peaks appear to include contributions from more than one level. This is apparent from inspection of the yield curves; the peaks are generally wider than the target thickness and show an increasing degree of overlapping. In addition, the angular distribution data show that peaks K, N, and P ($E_\alpha = 4\cdot658$, $4\cdot827$, and $4\cdot950$ MeV respectively) are definitely complex. For this reason no detailed analysis of the data for E_α greater than 4·6 MeV has been attempted.

The present results can be compared with those of Highland and Thwaites (1967) on the ^{20}Ne$(\alpha,\gamma)^{24}$Mg reaction. The appearance of the (α,γ) yield curve is quite distinct since it consists of a series of sharp peaks whose separation increases perceptibly above 4·6 MeV bombarding energy. With the exception of the peaks at $E_\alpha = 3\cdot997$ and $4\cdot483$ MeV, all the (α,γ) resonances are close in energy to prominent peaks in one or both of the ^{20}Ne$(\alpha,\alpha'\gamma_{1\cdot63})^{20}$Ne and ^{20}Ne$(\alpha,\mathrm{p}\gamma_{0\cdot44})^{23}$Na yield curves, although a number of these latter peaks appear to be complex. The levels seen in the ^{20}Ne$(\alpha,\gamma)^{24}$Mg reaction are presumably those with large values of Γ_α/Γ and Γ_γ. It appears that these levels contribute a significant, but not dominant, fraction of the ^{20}Ne$(\alpha,\alpha'\gamma_{1\cdot63})^{20}$Ne and ^{20}Ne$(\alpha,\mathrm{p}\gamma_{0\cdot44})^{23}$Na cross sections.

Below 4·6 MeV the peaks in the present data are generally well separated, and an attempt has been made to correlate these with levels observed in the ^{20}Ne$(\alpha,\gamma)^{24}$Mg and ^{23}Na+p reactions.

Peak B ($E_x = 12\cdot745$ MeV) appears clearly in both the 1·63 and 0·44 MeV data, and the angular distribution measurements give an unambiguous 2^+ assignment. It corresponds well to the 12·740 MeV 2^+ state observed by Highland and Thwaites (1967) in the ^{20}Ne$(\alpha,\gamma)^{24}$Mg reaction, and is probably the same level as that reported at $E_x = 12\cdot737$ MeV from ^{23}Na+p studies (Endt and Van der Leun 1962).

Peak D ($E_x = 12\cdot811$ MeV) appears clearly in the 1·63 MeV data and the angular distribution measurements give a definite 2^+ assignment. No corresponding peak is evident in the 0·44 MeV data; however, the close proximity of peaks C and E would make it difficult to resolve such a peak, and consequently the upper limit set on the appropriate partial width is relatively high (Table 4). It probably corresponds to the state observed at $E_x = 12\cdot805$ MeV in ^{23}Na+p (given a tentative 2^+ assignment by Stelson 1954; Baumann *et al.* 1956) and at $E_x = 12\cdot810$ MeV in ^{20}Ne$(\alpha,\gamma)^{24}$Mg (assigned 2^+ by Highland and Thwaites 1967).

Peak H ($E_x = 12\cdot978$ MeV) appears strongly in both sets of data. The angular distribution measurements indicate $J^\pi = 4^+$, 5^-, or 6^+. There is no obvious matching level in either the ^{23}Na+p or ^{20}Ne$(\alpha,\gamma)^{24}$Mg data. The results of Table 4 indicate that $(2J+1)\Gamma_{\alpha_1} \gtrsim 2050$ eV. Comparison with Wigner single-particle limits for $l' = 2$, 3, and 4 suggests that $J^\pi = 6^+$ is considerably less likely than $J^\pi = 4^+$ or 5^-. If the peaks H observed in the 0·44 and 1·63 MeV data do correspond to the same level then $(2J+1)\Gamma_{\mathrm{p}_1} \gtrsim 270$ eV; in this case $J^\pi = 6^+$ would be impossible, since the observed value of Γ_{p_1} would be many times larger than the Wigner limit. Thus the overall conclusion from the angular distribution and partial width data is that for the

$12 \cdot 978$ MeV level J^{π} is almost certainly 4^+ or 5^-, although a 6^+ assignment cannot be completely excluded.

Peaks A, G, and J correspond in energy to levels observed in ^{23}Na+p reactions at $E_x = 12 \cdot 659$ MeV (3^-), $12 \cdot 920$ MeV (1^-), and $13 \cdot 142$ MeV respectively and do not have any properties that would exclude identification with these levels.

The excitation energy and apparent width of peak C suggest that it may correspond to the $12 \cdot 779$ MeV level observed in the ^{23}Na(p, α_0)^{24}Mg reaction with $\Gamma = 30$ keV. However, this level is reported to have a negligible ^{23}Na(p, p$'\gamma_{0.44}$)^{23}Na yield and an observable ^{23}Na(p, γ)^{24}Mg yield (Prosser *et al.* 1956). If this is so, the suggested correspondence seems unlikely since peak C has an appreciable ^{20}Ne(α, p$\gamma_{0.44}$)^{23}Na yield and no yield was observed from ^{20}Ne(α, γ)^{24}Mg at the appropriate bombarding energy.

Peak I probably corresponds to the 2^+ level observed in ^{20}Ne(α, γ)^{24}Mg at $E_x = 13 \cdot 089$ MeV. The smallness of the yields of $1 \cdot 63$ MeV radiation at 0° and 90° is consistent with this spin and parity. The relative values of Γ_{α_1} and Γ_{p_1} show that it does not correspond to the $13 \cdot 088$ MeV (3^-) level observed in ^{23}Na+p reactions.

Thus, while many of the peaks observed for $4 \cdot 0 < E_\alpha < 4 \cdot 6$ MeV correspond to levels already observed in ^{23}Na+p reactions, a significant fraction are due to previously unobserved levels.

VII. Acknowledgments

The authors are grateful to Mr. R. V. Elliott, Dr. B. M. Sowerby, and Dr. B. V. Rao for assistance with some of the experimental work, to Dr. H. J. Hay for assistance with penetrability calculations, and to Dr. G. J. Highland and Dr. T. T. Thwaites for sending us their results prior to publication. One of us (I.F.W.) would like to thank Professor E. W. Titterton for his hospitality, and the Australian National University for the award of a Visiting Fellowship.

VIII. References

Bashkin, S., and Ophel, T. R. (1962).—*Nucl. Instrum.* **15**, 112.

Baumann, N. P., Prosser, F. W., Read, W. G., and Krone, R. W. (1956).—*Phys. Rev.* **104**, 377.

Endt, P. M., and Van der Leun, C. (1962).—*Nucl. Phys.* **34**, 1.

Highland, G., and Thwaites, T. T. (1967).—Pennsylvania State University preprint.

Kraus, A. A., Schiffer, J. P., Prosser, F. W., and Biedenharn, L. C. (1956).—*Phys. Rev.* **104**, 1667.

Ollerhead, R. W., and Kuehner, J. A. (1965).—Atomic Energy of Canada Ltd Rep. No. 2612, p. 13.

Prosser, F. W., Baumann, N. P., Brice, D. K., Read, W. G., and Krone, R. W. (1956).—*Phys. Rev.* **104**, 369.

Smulders, P. J. M. (1965).—*Physica* **31**, 973.

Stelson, P. H. (1954).—*Phys. Rev.* **96**, 1584.

Vivargent, M. (1959).—*Annls Phys.* **4**, 1047.

Yates, M. J. L. (1965).—"Alpha-, Beta-, and Gamma-ray Spectroscopy." (Ed. K. Siegbahn.) p. 1691. (North-Holland: Amsterdam.)